

Supporting Information

An Asymmetric Cryptand for the Site-Specific Coordination of 3d Metals in Multiple Oxidation States

Julia Jökel,^a Frauke Nyßen,^a Daniel Siegmund^b and Ulf-Peter Apfel*^{a,b}

^a Inorganic Chemistry I, Ruhr-Universität Bochum, Universitätsstr. 150, 44801 Bochum, Germany. E-mail: ulf-peter.apfel@rub.de, ulf-peter.apfel@umsicht.fraunhofer.de

^b Fraunhofer UMSICHT, Osterfelder Str. 3, 46047 Oberhausen, Germany.

Table of Content

1. NMR spectra.....	2
2. ESI-MS spectra.....	8
3. UV/vis/NIR spectra	9
4. EPR spectra.....	12
5. X-ray data	13

1. NMR spectra

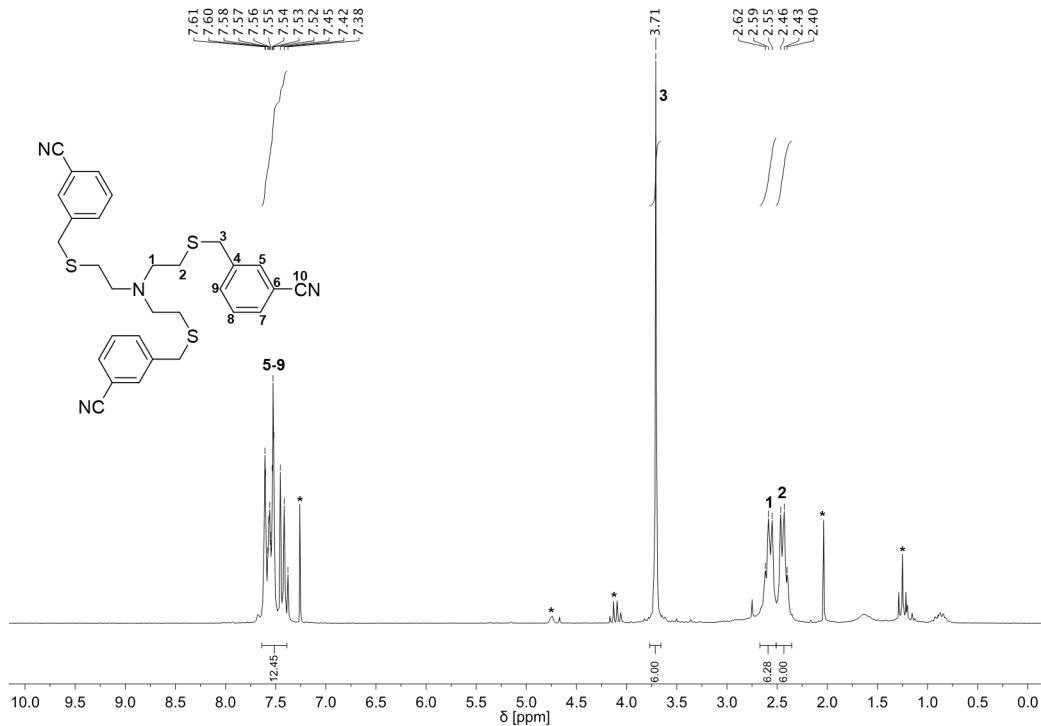


Figure S1. ^1H NMR spectrum (200 MHz, CDCl_3) of compound 3a.

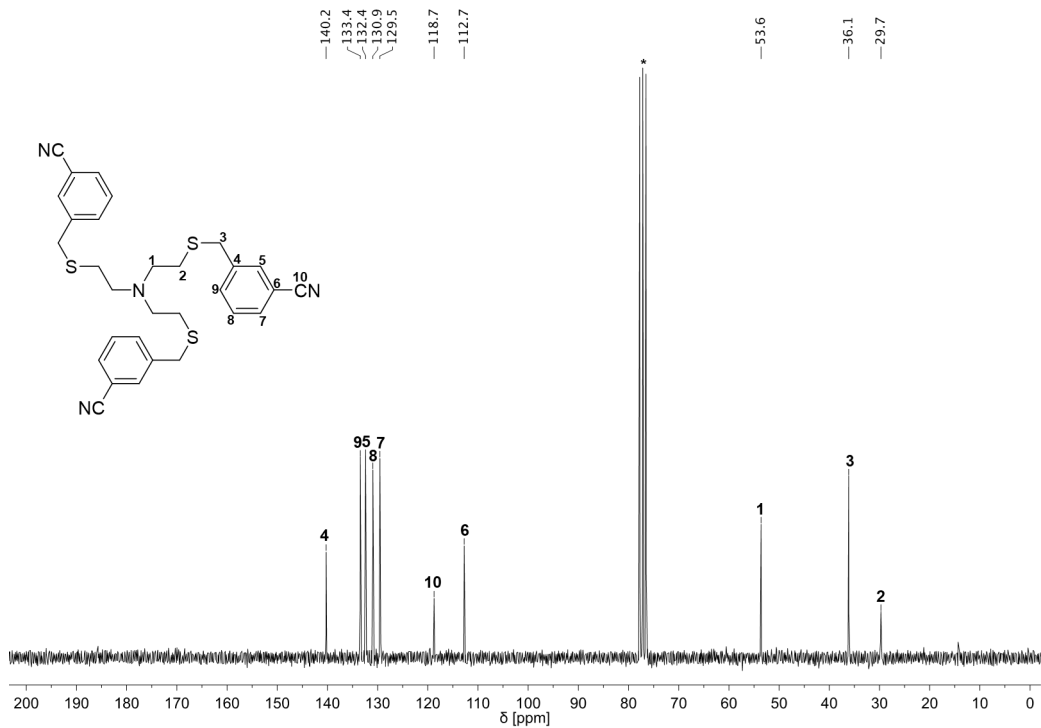


Figure S2. $^{13}\text{C}\{^1\text{H}\}$ NMR spectrum (50 MHz, CDCl_3) of compound 3a.

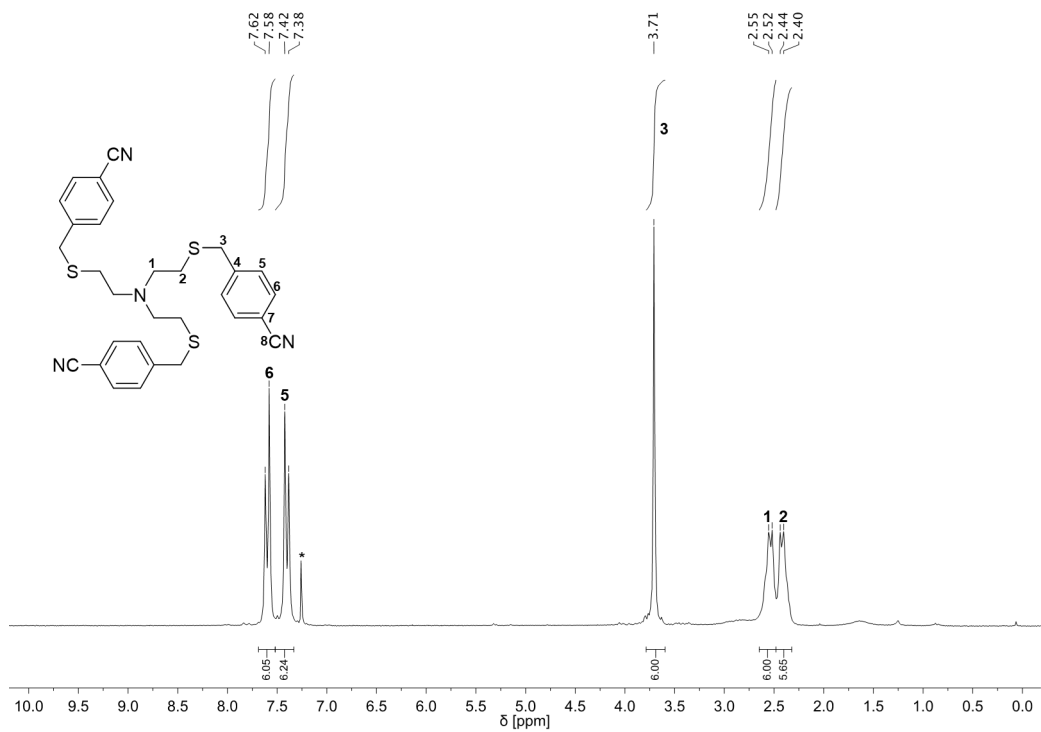


Figure S3. ^1H NMR spectrum (200 MHz, CDCl_3) of compound **3b**.

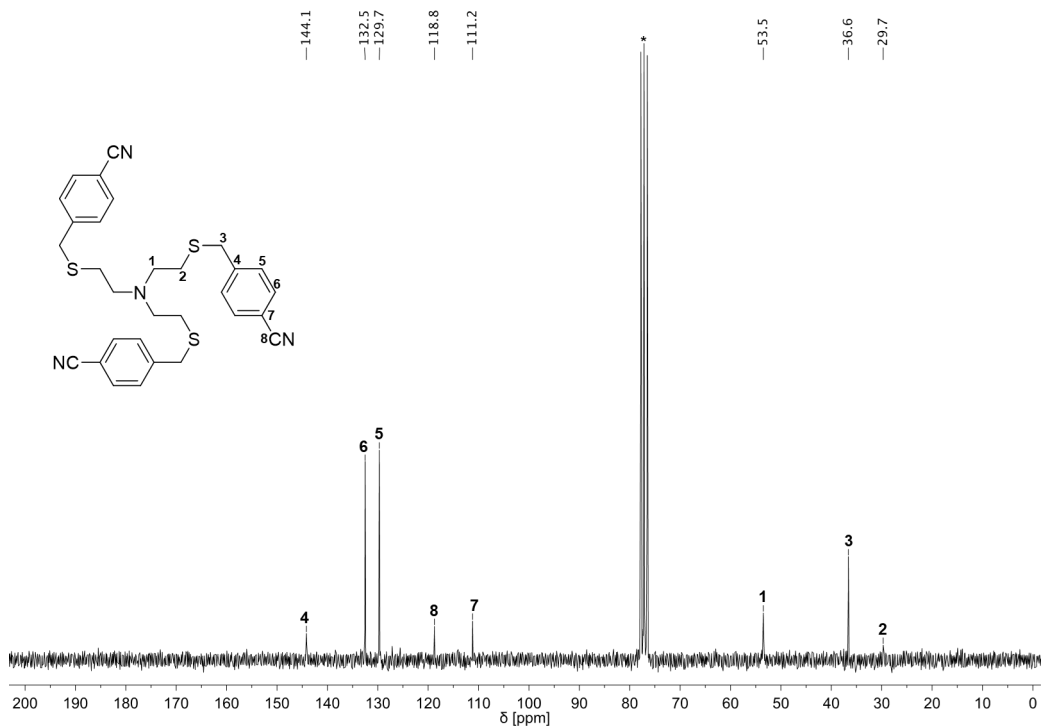


Figure S4. $^{13}\text{C}\{^1\text{H}\}$ NMR spectrum (50 MHz, CDCl_3) of compound **3b**.

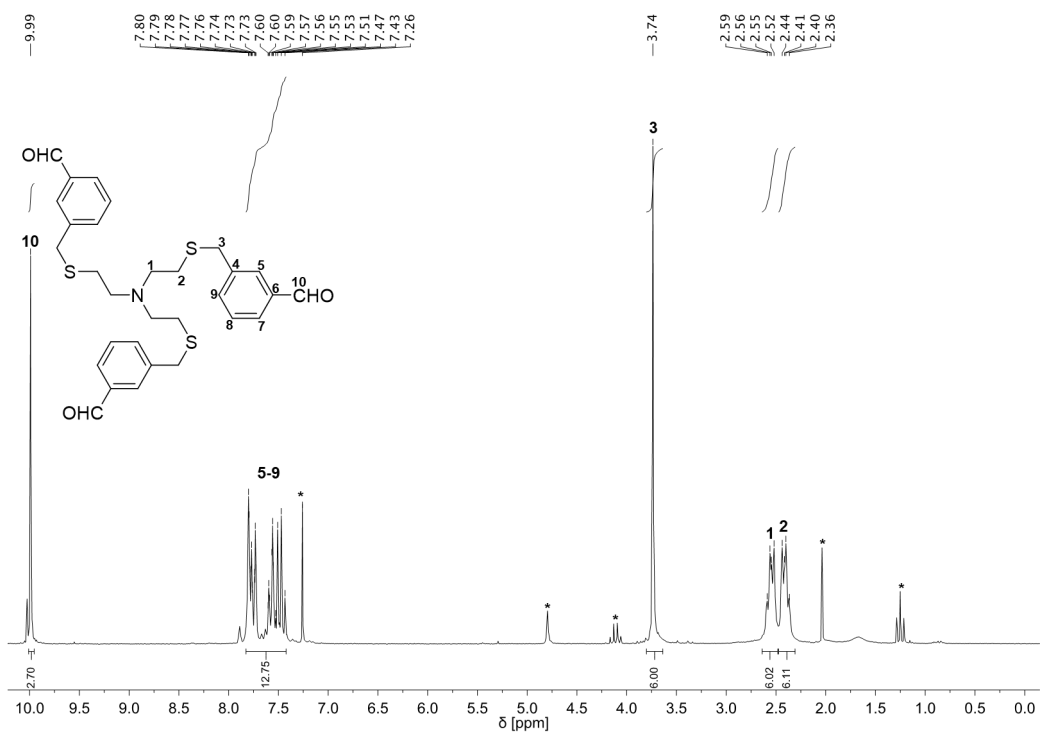


Figure S5. ^1H NMR spectrum (200 MHz, CDCl_3) of compound 4a.

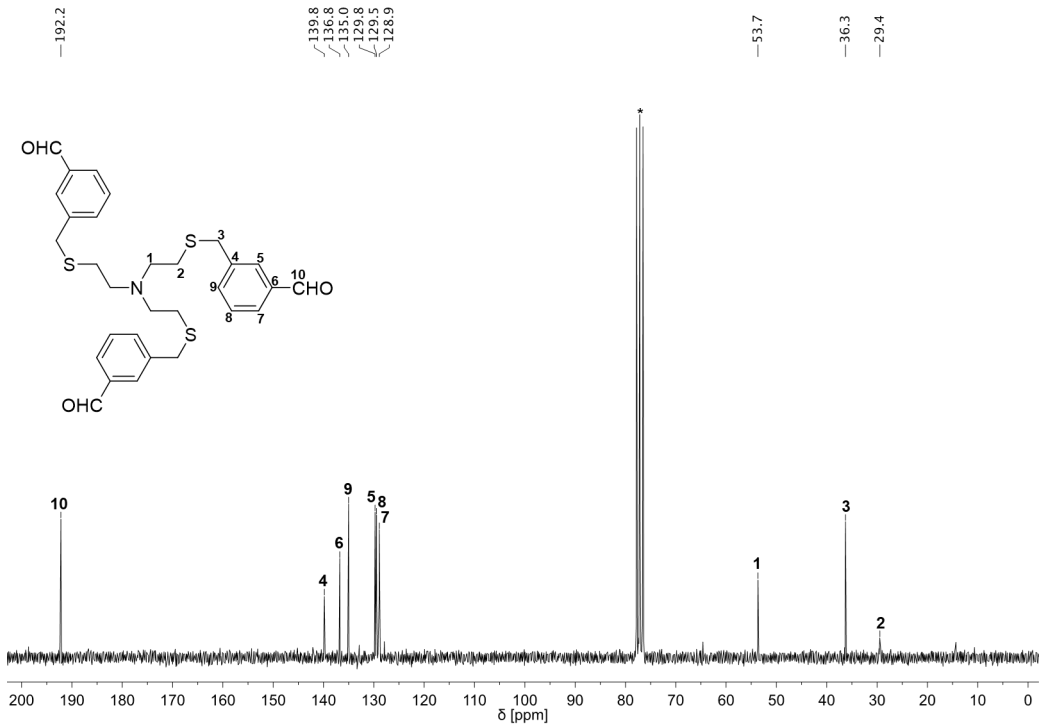


Figure S6. $^{13}\text{C}\{^1\text{H}\}$ NMR spectrum (50 MHz, CDCl_3) of compound 4a.

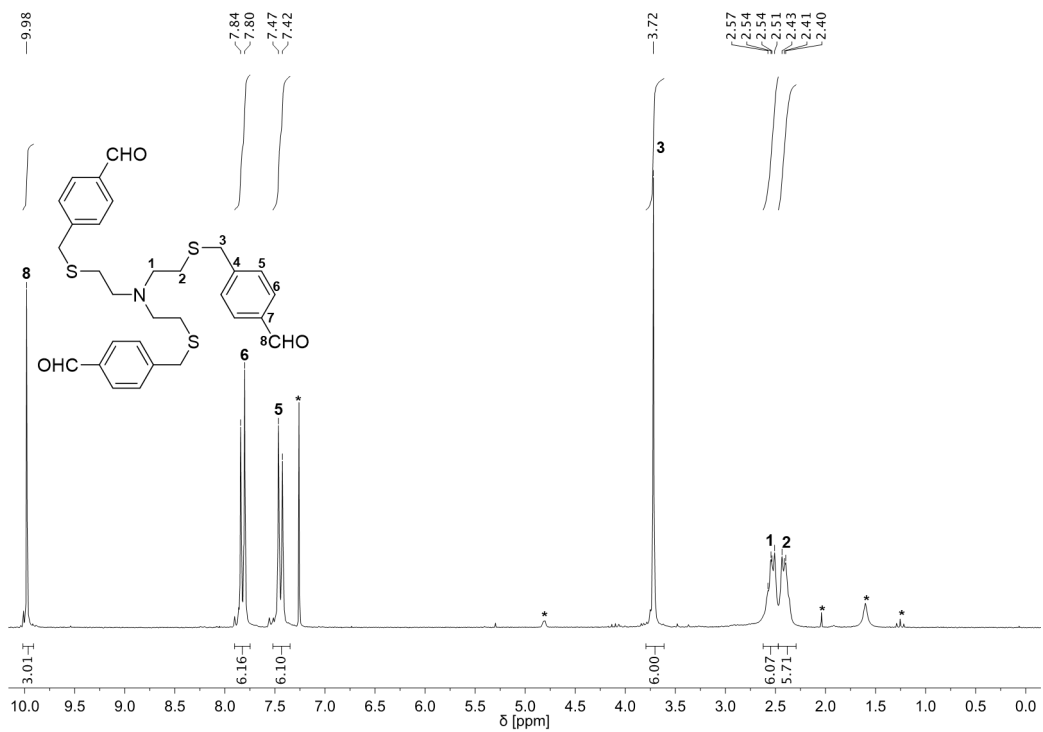


Figure S7. ^1H NMR spectrum (200 MHz, CDCl_3) of compound **4b**.

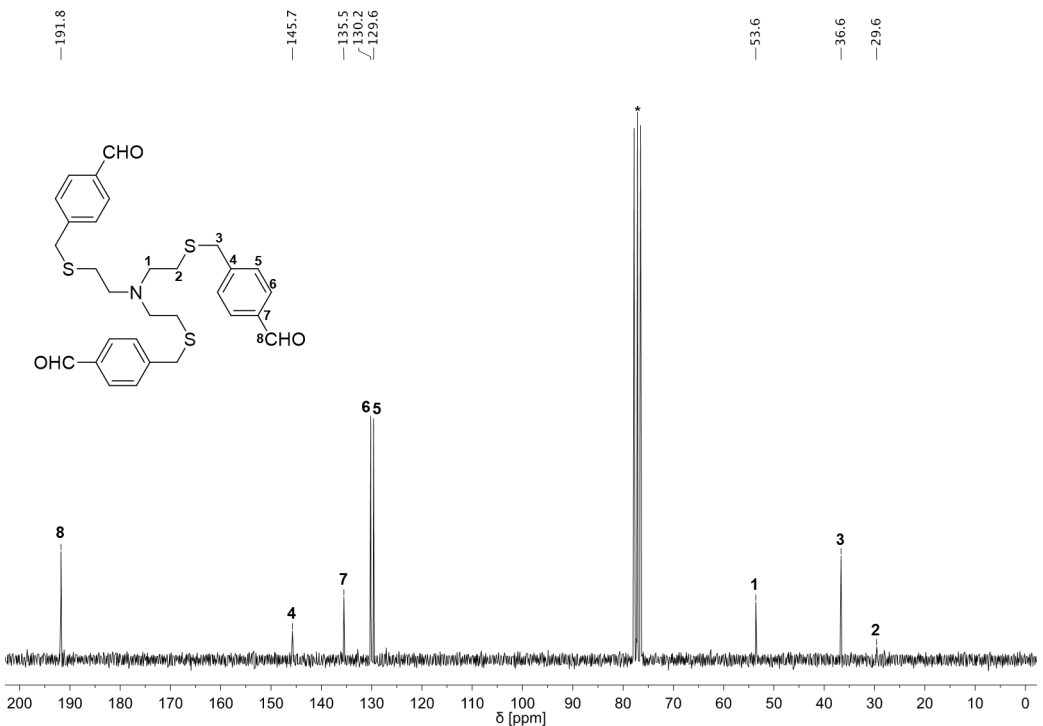


Figure S8. $^{13}\text{C}\{^1\text{H}\}$ NMR spectrum (50 MHz, CDCl_3) of compound **4b**.

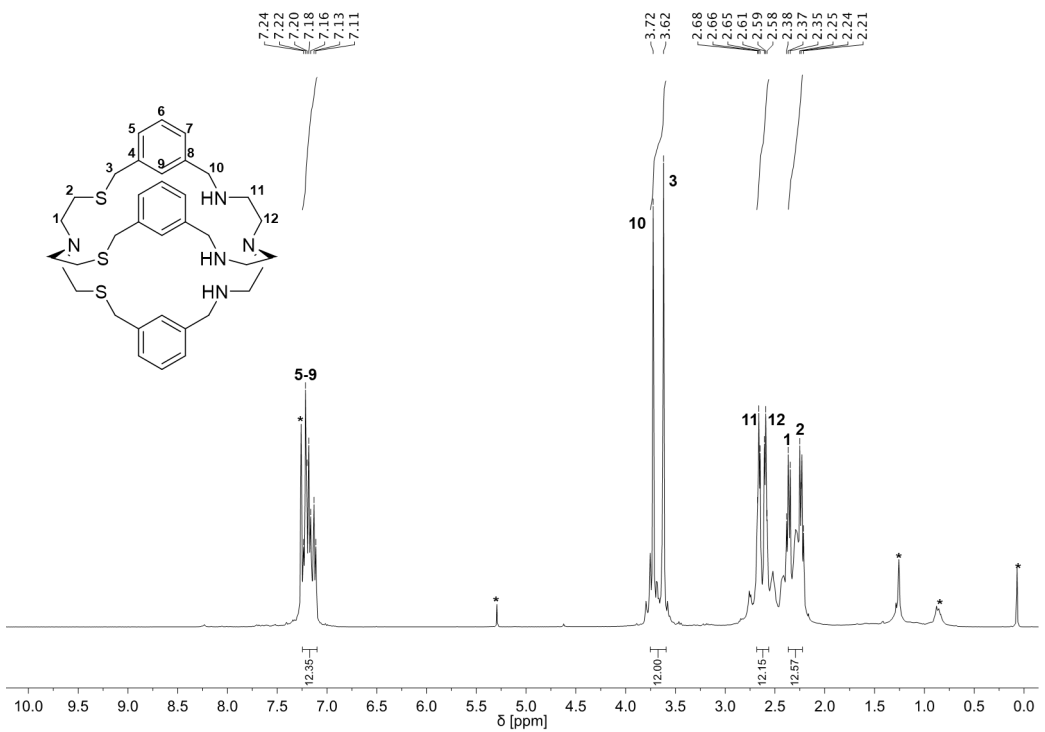


Figure S9. ^1H NMR spectrum (200 MHz, CDCl_3) of $\{\text{N}^{\text{S}},\text{N}^{\text{N}}\}_m$.

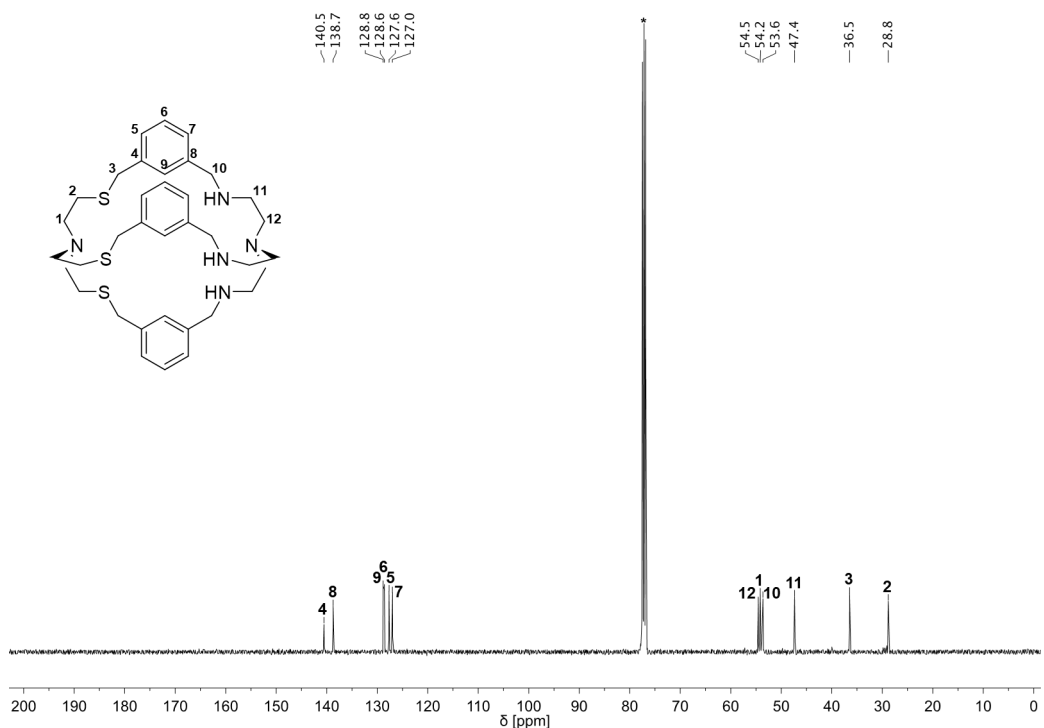


Figure S10. $^{13}\text{C}\{^1\text{H}\}$ NMR spectrum (50 MHz, CDCl_3) of $\{\text{N}^{\text{S}},\text{N}^{\text{N}}\}_m$.

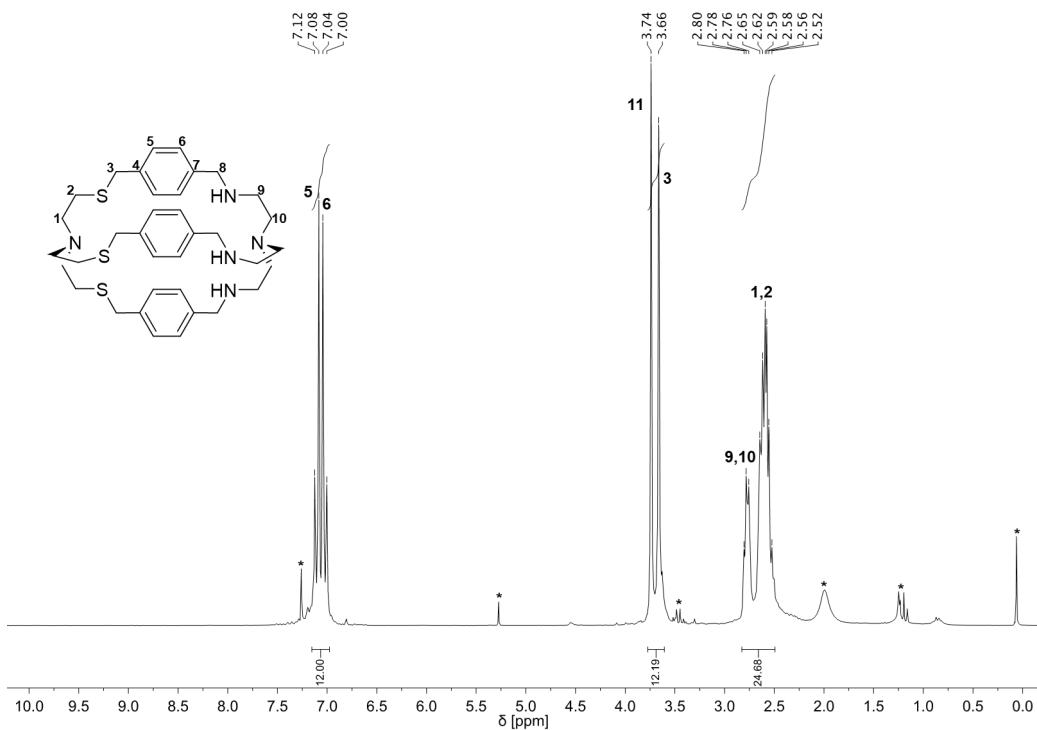


Figure S11. ^1H NMR spectrum (200 MHz, CDCl_3) of $\{\text{N}^{\text{S}},\text{N}^{\text{N}}\}_p$.

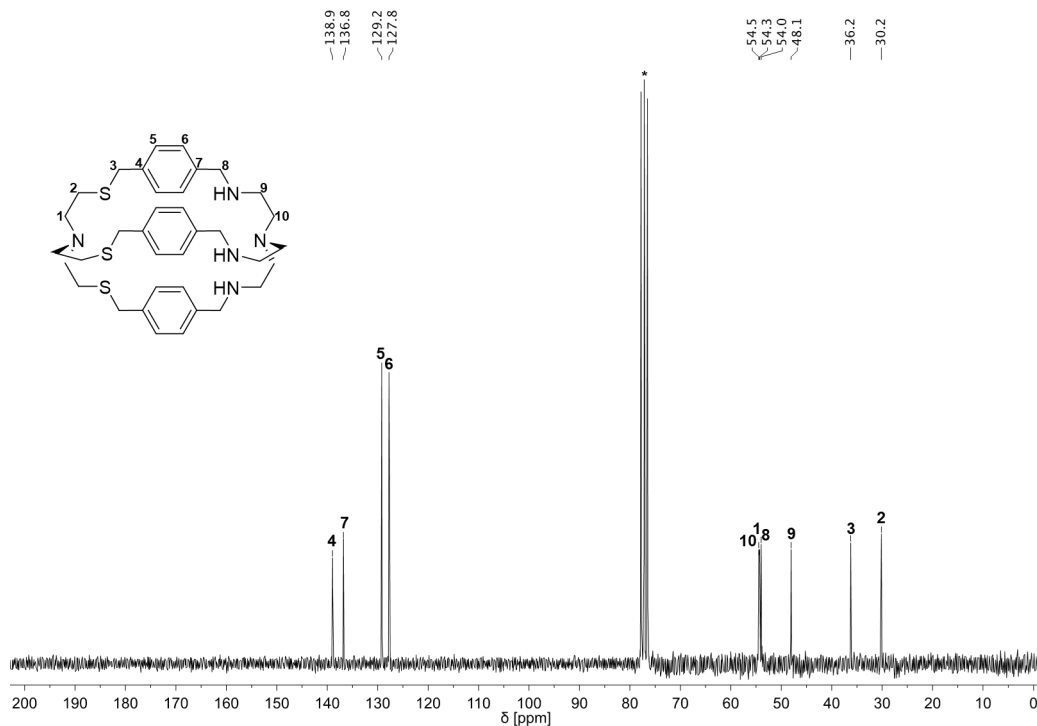


Figure S12. $^{13}\text{C}\{^1\text{H}\}$ NMR spectrum (50 MHz, CDCl_3) of $\{\text{N}^{\text{S}},\text{N}^{\text{N}}\}_p$.

2. ESI-MS spectra

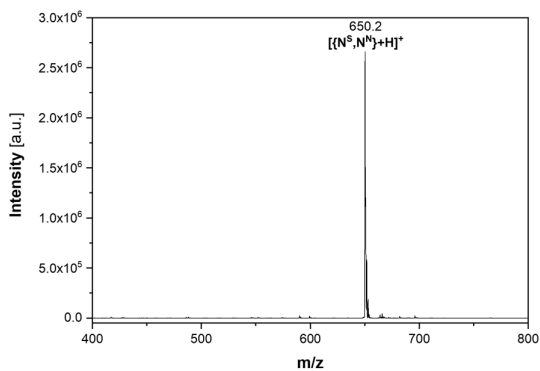


Figure S13. ESI-MS spectrum of $\{N^S, N^N\}$.

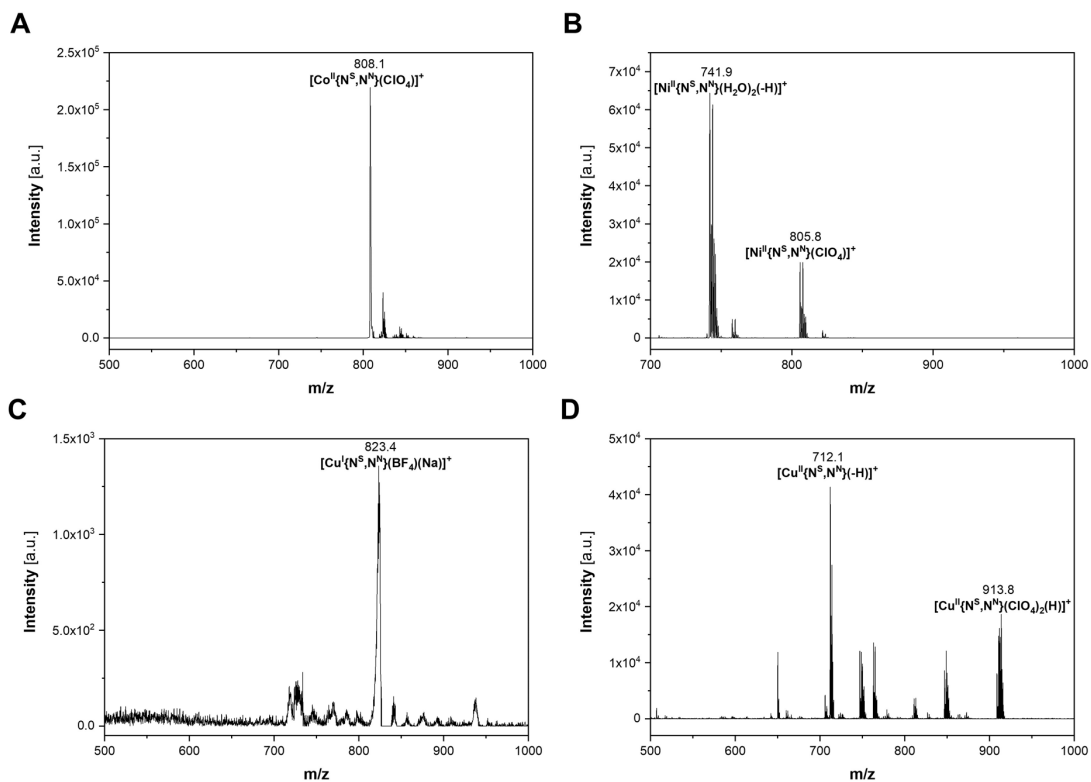


Figure S14. ESI-MS spectra of (A) $\text{Co}^{II}-\{N^S, N^N\}$, (B) $\text{Ni}^{II}-\{N^S, N^N\}$, (C) $\text{Cu}^{I}-\{N^S, N^N\}$ and (D) $\text{Cu}^{II}-\{N^S, N^N\}$.

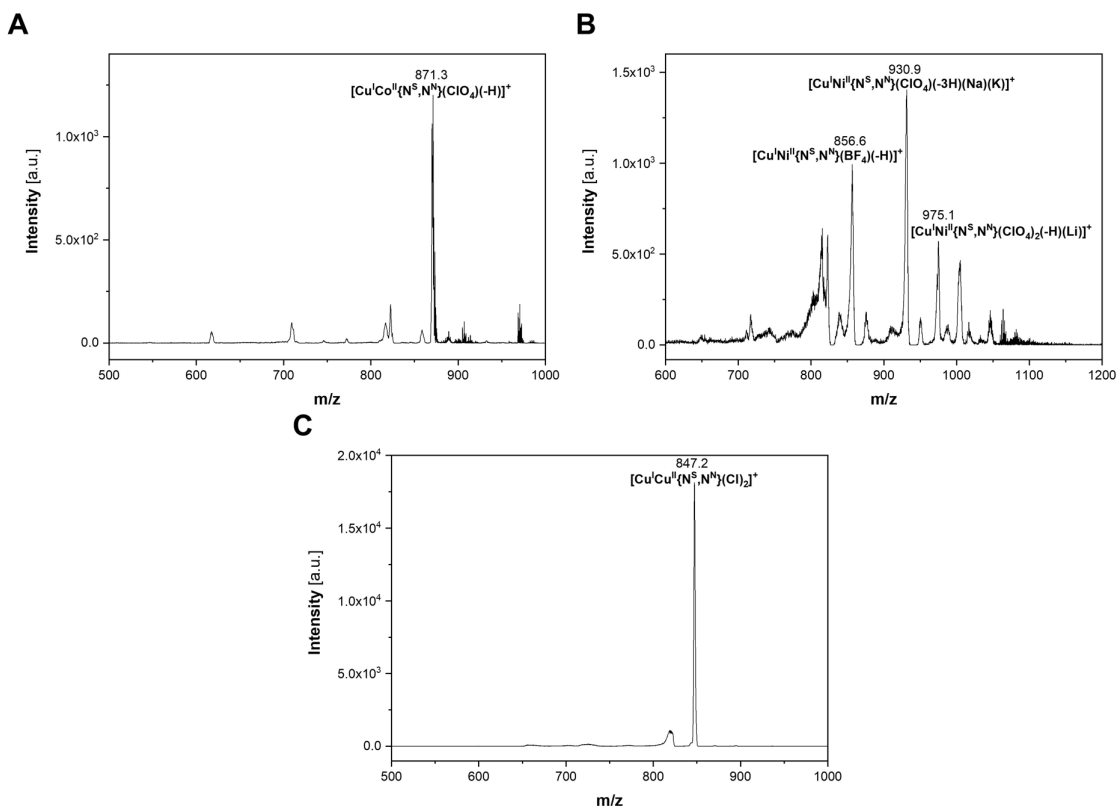


Figure S15. ESI-MS spectra of (A) $\text{Cu}^{\text{I}}\text{Co}^{\text{II}}\{-\text{N}^{\text{S}},\text{N}^{\text{N}}\}$, (B) $\text{Cu}^{\text{I}}\text{Ni}^{\text{II}}\{-\text{N}^{\text{S}},\text{N}^{\text{N}}\}$ and (C) $\text{Cu}^{\text{I}}\text{Cu}^{\text{II}}\{-\text{N}^{\text{S}},\text{N}^{\text{N}}\}$.

3. UV/vis/NIR spectra

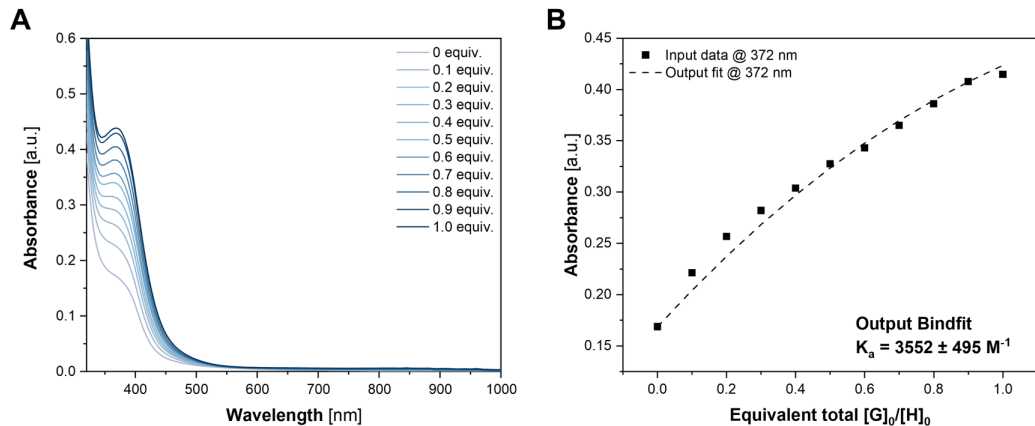


Figure S16. (A) UV/vis/NIR spectrum during the titration of a 0.011 M solution of $[\text{Cu}(\text{MeCN})_4](\text{BF}_4)$ to a 0.6 mM solution of $\{N^S, N^N\}$ in acetonitrile/methanol (4:1). (B) Fitting output from Bindfit for the determination of the association constant K_a . Data set and fitting results available online at: <http://app.supramolecular.org/bindfit/view/350887a5-85a2-4a93-911f-09b0cff0db3a>.

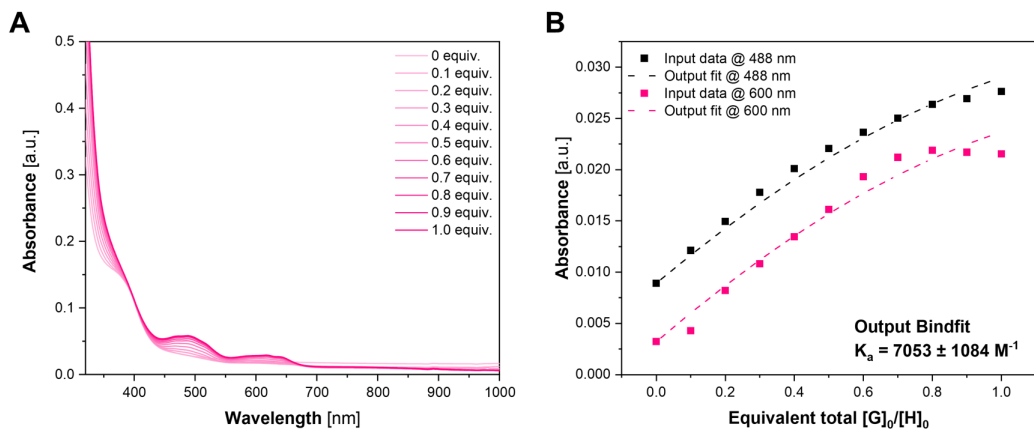


Figure S17. (A) UV/vis/NIR spectrum during the titration of a 0.011 M solution of $\text{Co}(\text{ClO}_4)_2 \cdot 6\text{H}_2\text{O}$ to a 0.6 mM solution of $\{\text{N}^{\text{S}}, \text{N}^{\text{N}}\}$ in acetonitrile/methanol (4:1). (B) Fitting output from Bindfit for the determination of the association constant K_a . Data set and fitting results available online at: <http://app.supramolecular.org/bindfit/view/7aee10be-d7dc-4005-ad96-80e3b7e7afb6>.

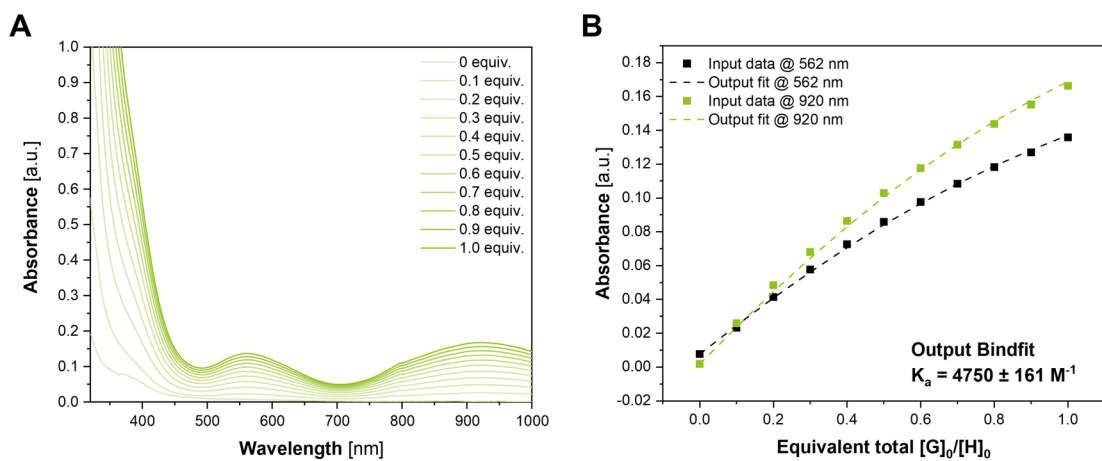


Figure S18. (A) UV/vis/NIR spectrum during the titration of a 0.011 M solution of $\text{Ni}(\text{ClO}_4)_2 \cdot 6\text{H}_2\text{O}$ to a 0.6 mM solution of $\{\text{N}^{\text{S}}, \text{N}^{\text{N}}\}$ in acetonitrile/methanol (4:1). (B) Fitting output from Bindfit for the determination of the association constant K_a . Data set and fitting results available online at: <http://app.supramolecular.org/bindfit/view/3e8aeb70-e9ae-4471-a78e-005ef804e01b>.

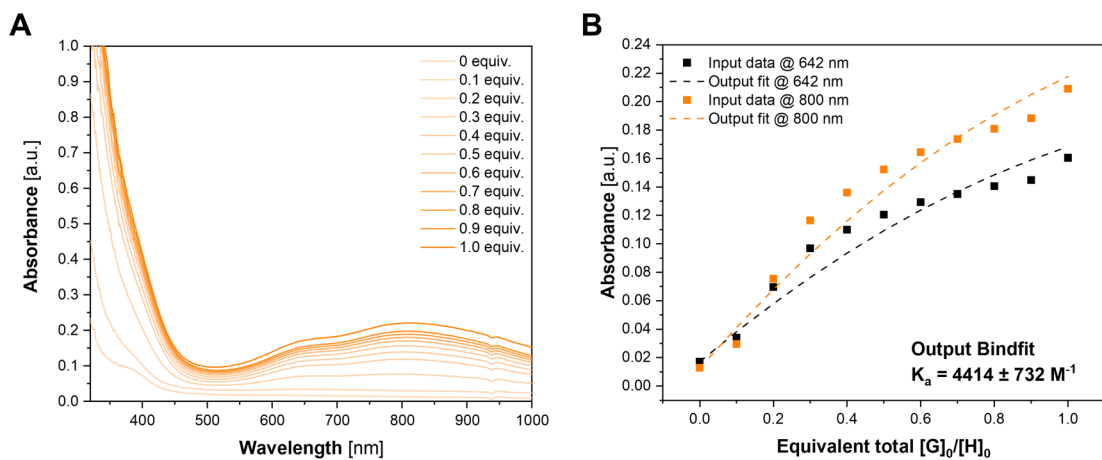


Figure S19. (A) UV/vis/NIR spectrum during the titration of a 0.011 M solution of CuCl_2 to a 0.6 mM solution of $\{\text{N}^{\text{S}}, \text{N}^{\text{N}}\}$ in acetonitrile/methanol (4:1). (B) Fitting output from Bindfit for the determination of the association constant K_a . Data set and fitting results available online at: <http://app.supramolecular.org/bindfit/view/bb5145d5-ab5b-4725-9f02-f7bbef465ea>.

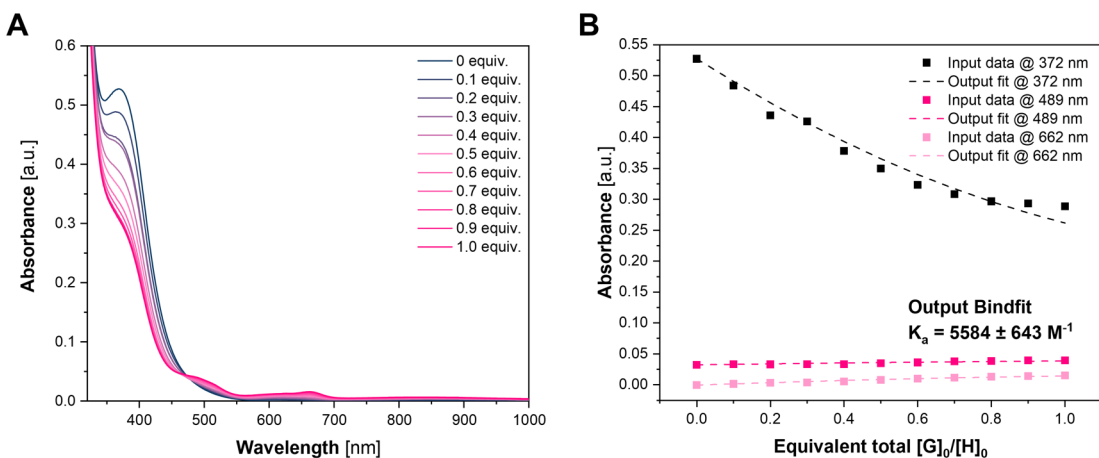


Figure S20. (A) UV/vis/NIR spectrum during the titration of a 0.011 M solution of $\text{Co}(\text{ClO}_4)_2 \cdot 6\text{H}_2\text{O}$ to a 0.6 mM solution of $\text{Cu}^{\text{I}}\text{-}\{\text{N}^{\text{S}},\text{N}^{\text{N}}\}$ in acetonitrile/methanol (4:1). (B) Fitting output from Bindfit for the determination of the association constant K_a . Data set and fitting results available online at: <http://app.supramolecular.org/bindfit/view/f8794315-7dee-4adc-918c-fe2528826d87>.

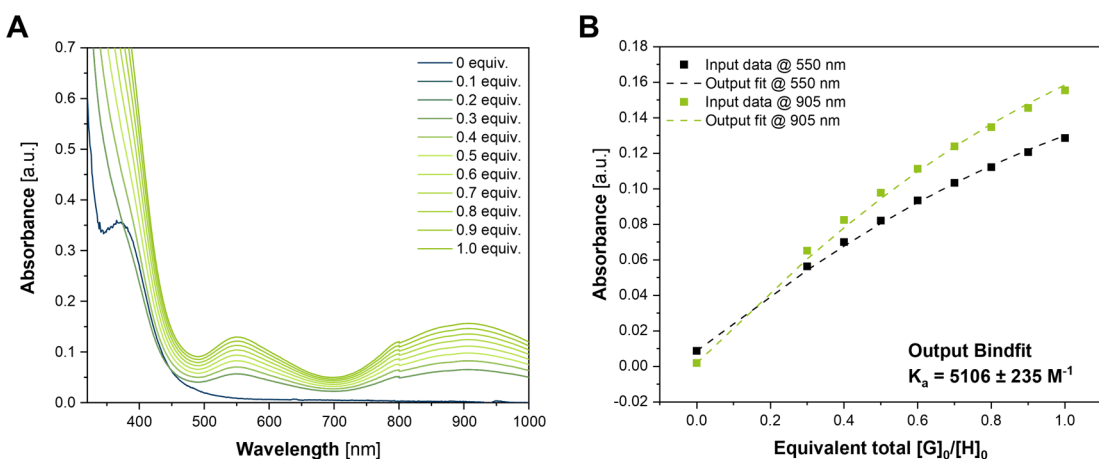


Figure S21. (A) UV/vis/NIR spectrum during the titration of a 0.011 M solution of $\text{Ni}(\text{ClO}_4)_2 \cdot 6\text{H}_2\text{O}$ to a 0.6 mM solution of $\text{Cu}^{\text{I}}\text{-}\{\text{N}^{\text{S}},\text{N}^{\text{N}}\}$ in acetonitrile/methanol (4:1). (B) Fitting output from Bindfit for the determination of the association constant K_a . Data set and fitting results available online at: <http://app.supramolecular.org/bindfit/view/32eb1e6c-b224-498f-a4e1-755828a22185>.

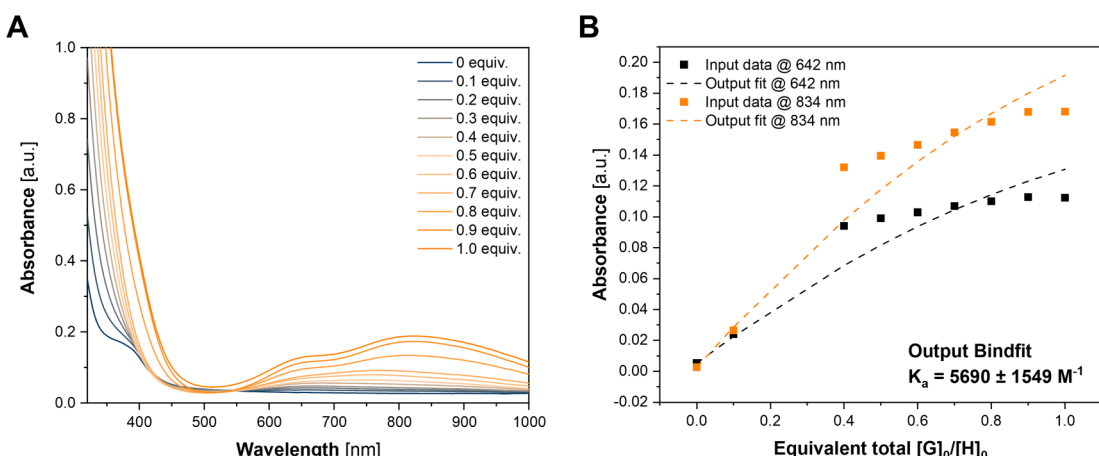


Figure S22. (A) UV/vis/NIR spectrum during the titration of a 0.011 M solution of CuCl_2 to a 0.6 mM solution of $\text{Cu}^{\text{I}}\text{-}\{\text{N}^{\text{S}},\text{N}^{\text{N}}\}$ in acetonitrile/methanol (4:1). (B) Fitting output from Bindfit for the determination of the association constant K_a . Data set and fitting results available online at: <http://app.supramolecular.org/bindfit/view/14bde302-5cf2-41d7-91fd-03582a76a606>.

4. EPR spectra

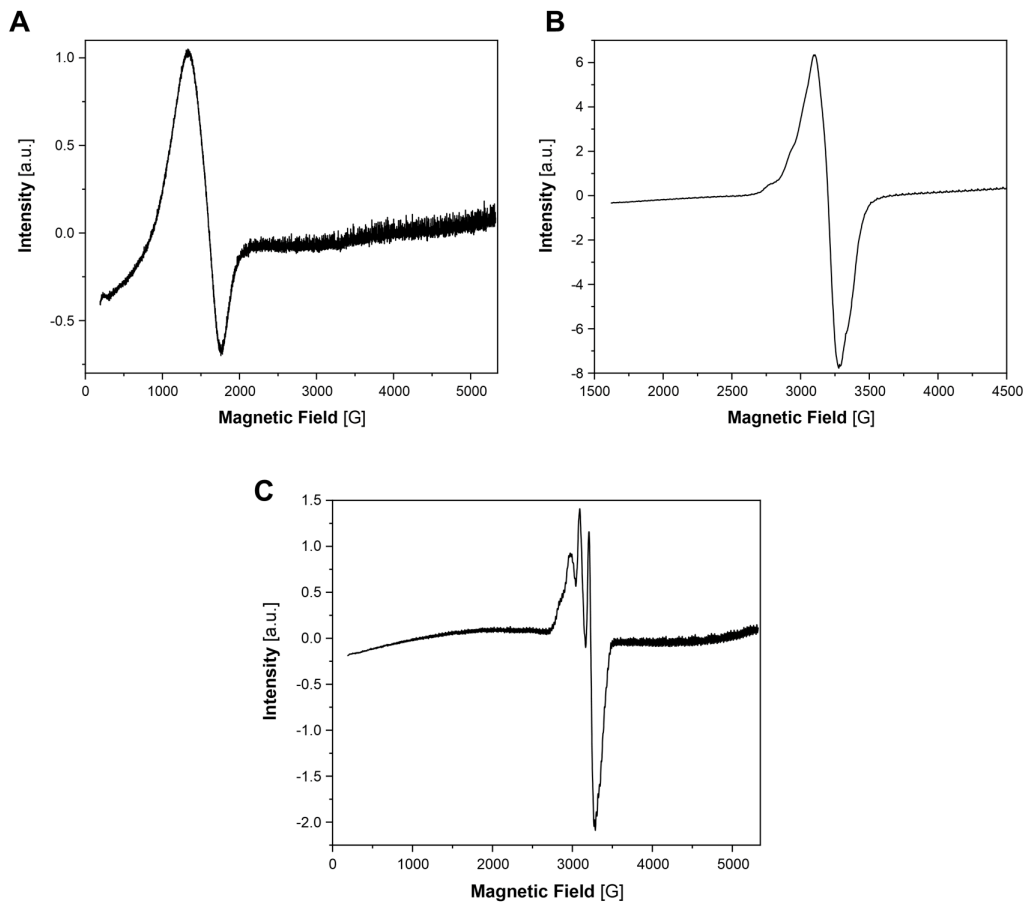


Figure S23. EPR spectra of (A) $\text{Co}^{\text{II}}\text{-}\{\text{N}^{\text{S}}, \text{N}^{\text{N}}\}$, (B) $\text{Cu}^{\text{II}}\text{-}\{\text{N}^{\text{S}}, \text{N}^{\text{N}}\}$ and (C) $\text{Cu}^{\text{I}}\text{-}\{\text{N}^{\text{S}}, \text{N}^{\text{N}}\}$ in frozen acetonitrile (1 mM).

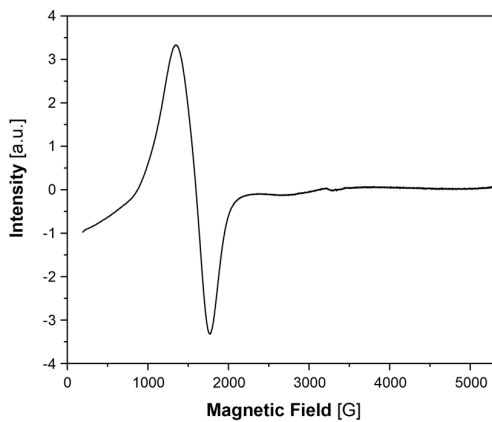


Figure S24. EPR spectrum of $\text{Co}^{\text{II}}\text{Co}^{\text{II}}\text{-}\{\text{N}^{\text{S}}, \text{N}^{\text{N}}\}$ in frozen acetonitrile (1 mM).

5. X-ray data

Table S1. Crystal data and structure refinement for $\{\text{N}^{\text{s}}, \text{N}^{\text{n}}\}_m(\text{ClO}_4)_4$ and $[\text{Ni}^{II}\{\text{N}^{\text{s}}, \text{N}^{\text{n}}\}_p(\text{CH}_3\text{CN})_2](\text{ClO}_4)_2$.

	$\{\text{N}^{\text{s}}, \text{N}^{\text{n}}\}_m(\text{ClO}_4)_4$	$[\text{Ni}^{II}\{\text{N}^{\text{s}}, \text{N}^{\text{n}}\}_p(\text{CH}_3\text{CN})_2](\text{ClO}_4)_2$
Empirical formula	$\text{C}_{36}\text{H}_{59}\text{Cl}_4\text{N}_5\text{O}_{18}\text{S}_3$	$\text{C}_{44}\text{H}_{63}\text{N}_9\text{O}_8\text{S}_3\text{Cl}_2\text{Ni}$
Formula weight [g mol⁻¹]	1087.86	1071.82
Temperature [K]	100	195(130)
Crystal system	monoclinic	triclinic
Space group	Cc	P-1
a [Å]	10.3506(5)	10.7050(2)
b [Å]	28.6229(14)	14.4139(3)
c [Å]	17.3038(8)	17.3426(3)
α [°]	90	77.4312(16)
β [°]	91.771(4)	87.3570(16)
γ [°]	90	73.3222(16)
V [Å³]	5124.0(4)	2501.60(8)
Z	4	2
ρ_{calc} [g cm⁻³]	1.410	1.423
μ [mm⁻¹]	0.425	3.209
F(000)	2280.0	1128.0
Radiation	MoK_α ($\lambda = 0.71073$)	CuK_α ($\lambda = 1.54184$)
2θ range for data collection [°]	6.162 to 49.992	6.522 to 149.344
	$-12 \leq h \leq 12$	$-13 \leq h \leq 13$
Index ranges	$-34 \leq k \leq 34$	$-18 \leq k \leq 18$
	$-20 \leq l \leq 20$	$-18 \leq l \leq 21$
Reflections collected	36004	45139
Independent reflections	8987 ($R_{\text{int}}=0.0441$)	10108 ($R_{\text{int}}=0.0211$)
Data/restraints/parameters	8987/107/635	10108/0/608
Goodness-of-fit on F^2	1.022	1.028
Final R indices [$I \geq 2\sigma(I)$]	$R_1=0.0434$, $wR_2=0.1083$	$R_1=0.0296$, $wR_2=0.0772$
Final R indices [all data]	$R_1=0.0498$, $wR_2=0.1145$	$R_1=0.0304$, $wR_2=0.0776$
Largest diff. peak/hole [e Å⁻³]	0.74/-0.56	0.77/-0.60

Table S2. Crystal data and structure refinement for $[\text{Cu}^{\text{II}}\{\text{N}^{\text{S}}, \text{N}^{\text{N}}\}_m](\text{Cl})_4$ and $[\text{Cu}^{\text{I}}\text{Cu}^{\text{II}}\{\text{N}^{\text{S}}, \text{N}^{\text{N}}\}_p(\text{CH}_3\text{OH})(\text{Cl})](\text{BF}_4)(\text{Cl})$.

	$[\text{Cu}^{\text{II}}\{\text{N}^{\text{S}}, \text{N}^{\text{N}}\}_m](\text{Cl})_4$	$[\text{Cu}^{\text{I}}\text{Cu}^{\text{II}}\{\text{N}^{\text{S}}, \text{N}^{\text{N}}\}_p(\text{CH}_3\text{OH})(\text{Cl})](\text{BF}_4)(\text{Cl})$
Empirical formula	$\text{C}_{76}\text{H}_{122}\text{Cl}_7\text{Cu}_2\text{N}_{10}\text{O}_4\text{S}_6$	$\text{C}_{41}\text{H}_{66}\text{BCl}_2\text{Cu}_2\text{F}_4\text{N}_6\text{O}_3\text{S}_3$
Formula weight [g mol⁻¹]	1807.42	1071.96
Temperature [K]	99.9(2)	99.95(10)
Crystal system	triclinic	orthorhombic
Space group	P-1	Pbca
a [Å]	12.4346(4)	18.53744(19)
b [Å]	13.9327(4)	17.36252(16)
c [Å]	15.5273(6)	30.7787(4)
α [°]	66.345(3)	90
β [°]	81.345(3)	90
γ [°]	69.195(3)	90
V [Å³]	2303.27(15)	9906.34(19)
Z	1	8
ρ_{calc} [g cm⁻³]	1.303	1.437
μ [mm⁻¹]	4.094	3.718
F(000)	953.0	4472.0
Radiation	CuK_{α} ($\lambda = 1.54184$)	CuK_{α} ($\lambda = 1.54184$)
2θ range for data collection [°]	7.326 to 134.996	7.466 to 149.438
	$-14 \leq h \leq 14$	$-21 \leq h \leq 23$
Index ranges	$-16 \leq k \leq 16$	$-21 \leq k \leq 21$
	$-15 \leq l \leq 18$	$-37 \leq l \leq 38$
Reflections collected	33145	94577
Independent reflections	8254 ($R_{\text{int}}=0.0243$)	10090 ($R_{\text{int}}=0.0416$)
Data/restraints/parameters	8254/6/490	10090/4/582
Goodness-of-fit on F²	1.232	1.023
Final R indices [$I \geq 2\sigma(I)$]	$R_1=0.0522, wR_2=0.1146$	$R_1=0.0352, wR_2=0.0921$
Final R indices [all data]	$R_1=0.0534, wR_2=0.1149$	$R_1=0.0432, wR_2=0.0990$
Largest diff. peak/hole [e Å⁻³]	0.71/-0.48	0.66/-0.62

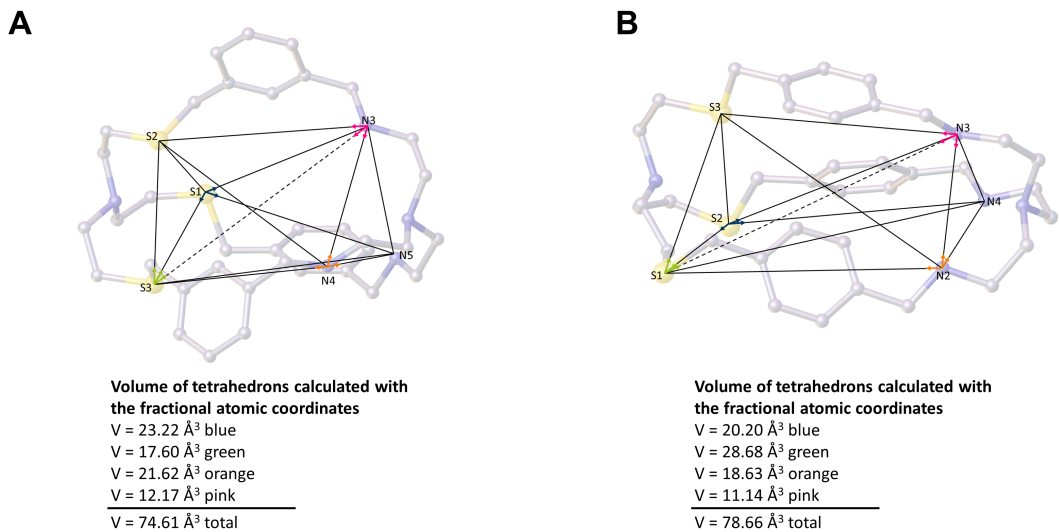


Figure S25. Molecular structures of (A) $\{N^S, N^N\}_m$ and (B) $\{N^S, N^N\}_p$. H atoms and counter ions are omitted for clarity. Color code: C grey, N blue, S yellow. The internal volume was estimated with a prism with three donor atoms of the individual binding sites as vertices. The prism was divided into four tetrahedrons and the volume was calculated using the common formula $V = \left| \frac{1}{6} \cdot \det(\vec{d}_1, \vec{d}_2, \vec{d}_3) \right|$ with the tension vectors $\vec{d}_1, \vec{d}_2, \vec{d}_3$.

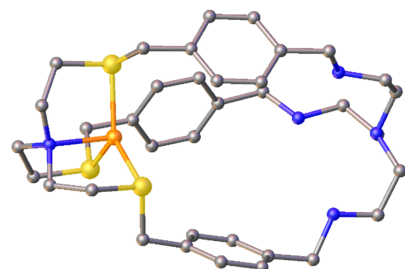


Figure S26. Molecular structures of $Cu^{+1}\{-N^S, N^N\}_p$. H atoms and counter ions are omitted for clarity. Color code: C grey, N blue, S yellow, Cu orange. X-ray data are of insufficient quality and therefore do not provide reliable information on bond lengths and angles and do not allow for a clear assignment of a +1 oxidation state of Cu.